A Sensitivity Study of Error Estimation in Reduced Elastic Multibody Systems ⋆

Joerg Fehr, Dennis Grunert *
Ashish Bhatt, Bernard Haasdonk **

* *ITM, University of Stuttgart, Pfaffenwaldring 9, 70569 Stuttgart (e-mail: [joerg.fehr,dennis.grunert]@itm.uni-stuttgart.de).*
** *IANS, University of Stuttgart, Pfaffenwaldring 57, 70569 Stuttgart, (e-mail: [ashish.bhatt,haasdonk]@mathematik.uni-stuttgart.de).*

Abstract: Error estimation is important for the further acceptance and usage of reduced order models to speed up simulations. We focus in this work on an a-posteriori error estimator for second-order mechanical systems which is valid for all model order reduction techniques based on Galerkin reduction. We analyze and improve this estimator in the following ways:
We conduct a sensitivity analysis of the error estimation on a beam model. It is shown that the estimator is sensitive to the reduction methods, the input functions, and the model itself. It is also shown that the overestimation can be arbitrary small.
Matrix norm inequalities are used to prevent inversion of the matrix. This results in an overall speedup of the error estimation routine as well as allows the scaling of the error estimator to larger systems, which was not possible before. Additionally, we present how the error estimator itself is plugged in a non-intrusive way to the Elastic Multibody simulation software Neweul-M^2 with least possible effort.

Keywords: Model Reduction, Error Estimation, Elastic Multibody Systems, A-Posteriori Error Estimation.

1. INTRODUCTION

Model order reduction (MOR) is an indispensable part within the simulation process of elastic multibody systems. Due to their modular structure, elastic multibody systems are especially suited to be used in a multiphysics / mechatronic simulation environment to model the mechanical part of such systems, see Fig. 1. One common formulation used to simulate elastic multibody systems is the floating frame of reference formulation (FFRF). Within this formulation, the motion $\boldsymbol{r}_\mathrm{P}$ of the point P of the i-th body is split into a large nonlinearly described motion of the reference frame K_i of the body and a linear modeled elastic motion $\boldsymbol{u}_\mathrm{P}$ with respect to the reference frame, see Fig. 1.

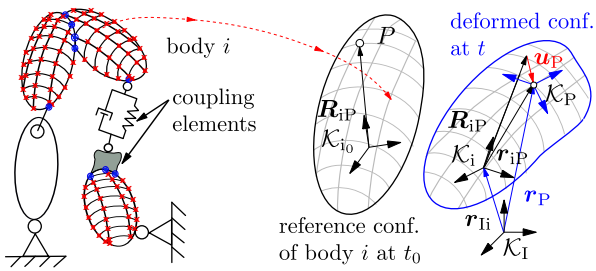

Fig. 1. EMBS and Floating Frame of Reference approach.

Therefore, one single elastic body is described with a nonlinear second order differential equation

$$\underbrace{\begin{bmatrix} m\boldsymbol{I} & m\tilde{\boldsymbol{r}}_\mathrm{c}^\mathrm{T} & \boldsymbol{C}_\mathrm{t}^\mathrm{T} \\ m\tilde{\boldsymbol{r}}_\mathrm{c} & \hat{\boldsymbol{I}} & \boldsymbol{C}_\mathrm{r}^\mathrm{T} \\ \boldsymbol{C}_\mathrm{t} & \boldsymbol{C}_\mathrm{r} & \boldsymbol{M}_\mathrm{e} \end{bmatrix}}_{\bar{\boldsymbol{M}}_\mathrm{i}} \underbrace{\begin{bmatrix} \ddot{\boldsymbol{q}}_\mathrm{t} \\ \ddot{\boldsymbol{q}}_\mathrm{r} \\ \ddot{\boldsymbol{q}}_\mathrm{e} \end{bmatrix}}_{\boldsymbol{z}_{\mathrm{III\,i}}} + \underbrace{\begin{bmatrix} \boldsymbol{0} \\ \boldsymbol{0} \\ \boldsymbol{k}_\mathrm{ee} \end{bmatrix}}_{\boldsymbol{k}_{\mathrm{e\,i}}} = \underbrace{\begin{bmatrix} \boldsymbol{k}_\mathrm{at} \\ \boldsymbol{k}_\mathrm{ar} \\ \boldsymbol{k}_\mathrm{ae} \end{bmatrix}}_{\boldsymbol{k}_{\mathrm{a\,i}}} \tag{1}$$

which is divided into three parts, low-dimensional translational and rotational parts and high-dimensional elastic part. The force vector $\boldsymbol{k}_{\mathrm{a}\{\mathrm{t,r,e}\}\,\mathrm{i}}$ consists of centrifugal, Coriolis, volumetric, surface and external point forces and point moments. Often, the internal elastic force $\boldsymbol{k}_{\mathrm{e\,i}}$ is approximated by $\boldsymbol{k}_\mathrm{ee} \approx \boldsymbol{K}_\mathrm{e}\boldsymbol{q}_\mathrm{e} + \boldsymbol{D}_\mathrm{e}\dot{\boldsymbol{q}}_\mathrm{e}$. The lower part of Eq. (1) corresponds to the large system of elastic deformations, where $\boldsymbol{q}_\mathrm{e} \in \mathbb{R}^N$ is the elastic coordinate vector which is used to approximate the elastic deformation $\boldsymbol{u}$ of body i at point $\boldsymbol{R}$ and time t by a Ritz approach $\boldsymbol{u}(\boldsymbol{R},t) \approx \boldsymbol{\Phi}(\boldsymbol{R})\boldsymbol{q}_\mathrm{e}(t)$. The deformation expressed by the linear elasticity approach is coupled with $\boldsymbol{C}_\mathrm{t} \in \mathbb{R}^{N\times 3}$ and $\boldsymbol{C}_\mathrm{r} \in \mathbb{R}^{N\times 3}$ to the nonlinear rigid body part.

In a first approximation, only the lower right part of the nonlinear ODE (1) is viewed as a linear time invariant multiple-input multiple-output (MIMO) system:

$$\begin{aligned} \boldsymbol{M}_\mathrm{e}\ddot{\boldsymbol{q}}_\mathrm{e}(t) + \boldsymbol{D}_\mathrm{e}\dot{\boldsymbol{q}}_\mathrm{e}(t) + \boldsymbol{K}_\mathrm{e}\boldsymbol{q}_\mathrm{e}(t) &= \boldsymbol{B}_\mathrm{e}\boldsymbol{u}_\mathrm{e}(t), \\ \boldsymbol{y}_\mathrm{e}(t) &= \boldsymbol{C}_\mathrm{e}\boldsymbol{q}_\mathrm{e}(t). \end{aligned} \tag{2}$$

The subparts of the equation are explained, e.g., in Fehr (2011). However, it is important to mention that the external forces and the coupling forces to the nonlinear rigid body motion, $\boldsymbol{C}_\mathrm{t}\ddot{\boldsymbol{q}}_\mathrm{t} + \boldsymbol{C}_\mathrm{r}\ddot{\boldsymbol{q}}_\mathrm{r}$, are considered as inputs $\boldsymbol{u}_\mathrm{e}(t) \in \mathbb{R}^p$ by the control matrix $\boldsymbol{B}_\mathrm{e} \in \mathbb{R}^{N\times p}$. Furthermore, the output $\boldsymbol{y}_\mathrm{e}(t) \in \mathbb{R}^r$ captures deformations of

⋆ The authors would like to thank the German Research Foundation (DFG) for financial support FE 1583/2-1 and HA 5821/5-1 of the project at the University of Stuttgart

interest via the observation matrix $\boldsymbol{C}_\mathrm{e} \in \mathbb{R}^{r\times N}$ which can be chosen arbitrarily.

This linear second order MIMO system is reduced separately for every body by appropriate second order structure preserving reduction techniques, e.g., by a Petrov-Galerkin ansatz $\boldsymbol{q}_\mathrm{e}(t) \approx \boldsymbol{V}\bar{\boldsymbol{q}}(t)$, where $\bar{\boldsymbol{q}} \in \mathbb{R}^n$, $\boldsymbol{V} \in \mathbb{R}^{N\times n}$ and $n \ll N$.

However, the reduced linear MIMO system is never simulated. Instead, $\boldsymbol{V}$ is used in Eq. (1) to calculate a reduced nonlinear ODE for one elastic body

$$\begin{bmatrix} m\boldsymbol{I} & & \text{sym.} \\ m\tilde{\boldsymbol{r}}_\mathrm{c}(\bar{\boldsymbol{q}}) & \hat{\boldsymbol{I}}(\bar{\boldsymbol{q}}) & \\ \bar{\boldsymbol{C}}_\mathrm{t}(\bar{\boldsymbol{q}}) & \bar{\boldsymbol{C}}_\mathrm{r}(\bar{\boldsymbol{q}}) & \bar{\boldsymbol{M}} \end{bmatrix} \begin{bmatrix} \ddot{\boldsymbol{q}}_\mathrm{t} \\ \ddot{\boldsymbol{q}}_\mathrm{r} \\ \ddot{\bar{\boldsymbol{q}}} \end{bmatrix} + \begin{bmatrix} \boldsymbol{0} \\ \boldsymbol{0} \\ \bar{\boldsymbol{K}}\bar{\boldsymbol{q}} + \bar{\boldsymbol{D}}\dot{\bar{\boldsymbol{q}}} \end{bmatrix} = \begin{bmatrix} \bar{\boldsymbol{k}}_\mathrm{at} \\ \bar{\boldsymbol{k}}_\mathrm{ar} \\ \bar{\boldsymbol{k}}_\mathrm{ae} \end{bmatrix} \quad (3)$$

which now depends on the reduced coordinates $\bar{\boldsymbol{q}}$. Here $\bar{\boldsymbol{C}}_\mathrm{t} = \boldsymbol{V}^T\boldsymbol{C}_\mathrm{t}, \bar{\boldsymbol{C}}_\mathrm{r} = \boldsymbol{V}^T\boldsymbol{C}_\mathrm{r}, \bar{\boldsymbol{M}} = \boldsymbol{V}^T\boldsymbol{M}_\mathrm{e}\boldsymbol{V}, \bar{\boldsymbol{K}} = \boldsymbol{V}^T\boldsymbol{K}_\mathrm{e}\boldsymbol{V}$, and $\bar{\boldsymbol{D}} = \boldsymbol{V}^T\boldsymbol{D}_\mathrm{e}\boldsymbol{V}$. Furthermore, the terms $\bar{\boldsymbol{k}}$, $\hat{\boldsymbol{I}}$, and $\tilde{\boldsymbol{r}}_\mathrm{c}$ may also depend on the reduced coordinate and are calculated based on the space spanned by the matrix $\boldsymbol{V}$, see Fehr (2011).

Error Estimation Methods Within this simulation process, multiple approximations are made and every approximation introduces an error. For example, the residual

$$\boldsymbol{R}_\mathrm{m}(t) = \boldsymbol{M}_\mathrm{e}\boldsymbol{V}\ddot{\bar{\boldsymbol{q}}}(t) + \boldsymbol{D}_\mathrm{e}\boldsymbol{V}\dot{\bar{\boldsymbol{q}}}(t) + \boldsymbol{K}_\mathrm{e}\boldsymbol{V}\bar{\boldsymbol{q}}(t) - \boldsymbol{B}_\mathrm{e}\boldsymbol{u}_\mathrm{e}(t), \quad (4)$$

represents the error induced by the reduction of the original second order MIMO system with a reduced second order system. This linear error of the elastic part also introduces an error in the overall nonlinear system.

But without information about the approximation error, the simulation results cannot be trusted anymore. Calculation of the real error involves an evaluation of the original system which is not feasible for large-scale systems. The importance of error estimation for MOR has led to various error estimation techniques; see, e.g., Panzer (2014) for frequency domain errors or Gubisch and Volkwein (2017) for a-priori time-domain error bounds. Research for Elastic Multibody Systems (EMBS) is currently investigated. We will focus in the following on second order MIMO systems but already implemented our findings in an EMBS framework. While a-priori error bounds give worst-case behavior bounds but ensure good approximation independent of the simulation setting, the individual simulation runs could be much better than this worst case. This means that the a-priori error bounds might be largely overestimating the actual error. Therefore, a-posteriori error control as explained in Haasdonk and Ohlberger (2011); Ruiner et al. (2012) are used, examined and extended in this work. One advantage of a-posteriori error control is that the reduced model should give additional error information for its current simulation setting of the reduced system for each special input signal, loading case, parameter etc. This allows to create adaptive simulations, in which the accuracy of the reduced model is adapted if the reduction error is too large. It is the goal of this paper to analyze this error estimator in more detail and provide improvements regarding the computation speed.

Another common approach to modeling elastic multibody systems is absolute coordinate formulation (ACF). In contrast to FFRF, ACF uses global coordinates also for elastic degrees of freedom of the system. This leads to a system of the form (1) with a constant mass matrix. An investigation of ACF and MOR error incurred therein is presented in Bhatt et al. (2017).

The next section describes the model investigated in our analysis and the simulation framework. This is followed by a possible speedup with matrix inequalities and a sensitivity analysis of the error estimator. We will also show how the estimator is implemented in a non-intrusive and easy to use manner within, e.g., Neweul-M^2.

2. EXAMPLE AND INVOLVED PROGRAMS

The error bounds are developed here only for the linear elastic part with the help of a small academic example, a two-link elastic manipulator with slender arms, see Fig. 2.

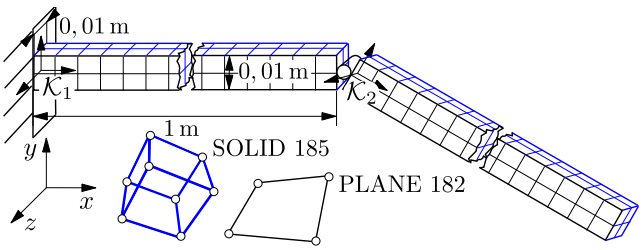

Fig. 2. Two link elastic manipulator with slender arms. The system is modeled either with plane stress 2D-plane element (black, PLANE182 in ANSYS) or with eight nodes hexahedron elements (blue, SOLID185 in ANSYS). Two tangent frames located at the outer left are used as reference frames.

As shown in Fig. 3, Morembs is used in a first step to extract the FE data from a commercial FE software ANSYS from ANSYS Inc. in our example. Morembs is a MOR software package for second order mechanical systems with various import and export capabilities to EMBS and FE solvers developed at the Institute of Engineering and Computational Mechanics, see Fehr et al. (2017). As explained in Fehr (2011), all parts in (1) can be calculated from the system data of a free FE body. The data is now available in Morembs but is also accessible for RBmatlab, a MOR software package based on the Reduced Basis approach and developed at the Institute of Applied Analysis and Numerical Simulation, see Haasdonk (2017). This simple example of a two-link elastic manipulator with slender arms (see Fig. 2) is chosen since it can be modeled both in Morembs, which uses reduction methods based on system matrices like Krylov and Gramian-based methods, as well as in RBmatlab, which uses data based reduction like POD. This way, we can compare the results via a common interface for validation.

In a next step the elastic projector, necessary to compute all parts in (3), is calculated by finding a good approximation $\boldsymbol{V}$ of the second-order MIMO system (2). Furthermore, a symplectic basis (see Maboudi Afkham and Hesthaven (2017)) can be calculated with RBmatlab by using simulation data snapshots. Afterwards, Morembs creates the projected data describing the elastic body to be used in a reduced EMBS simulation. Within the reduced EMBS simulation executed in Neweul-M^2, the

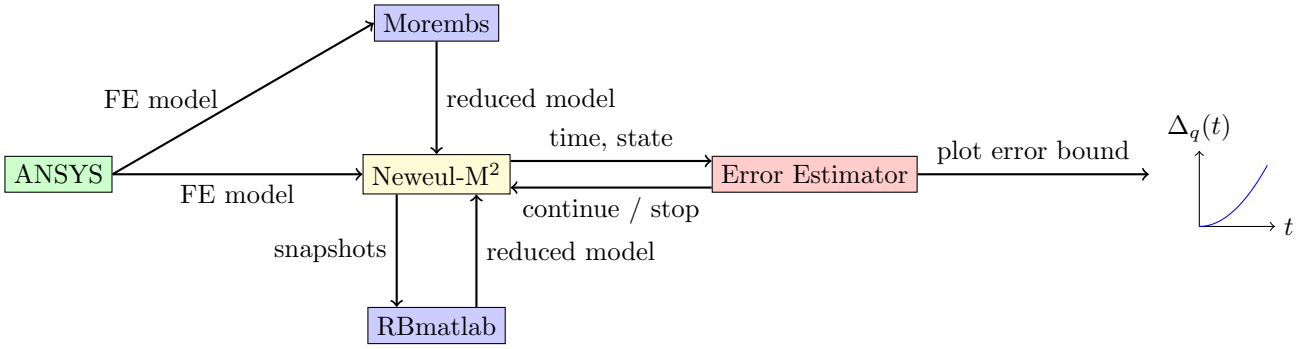

Fig. 3. Involved programs and workflow: The FE model from ANSYS is either reduced directly (based on the system matrices) in Morembs or used in Neweul-M^2 for snapshot generation. These snapshots can then be used in RBmatlab to generate a reduced model. Either way, the reduced model is simulated in Neweul-M^2. In parallel to the simulation, the error is estimated in a separate Matlab class and used to decide if the simulation should continue or abort.

error estimator runs in parallel as will be described later. Neweul-M^2 is a software package written in Matlab for the dynamic analysis of mechanical systems in the elastic multibody setting described above, see Kurz et al. (2010).

3. ERROR ESTIMATOR AND IMPROVEMENTS

In this section, we will introduce the error estimator by Ruiner et al. (2012) and present our improvements to it.

3.1 Original Error Estimator

For single linear FE bodies, an a-posteriori error estimator for second order mechanical systems is given in Ruiner et al. (2012). The error for the position states of the elastic part is given as

$$\begin{aligned}\boldsymbol{e}_{\mathrm{m}}(t) &= \boldsymbol{\Phi}_{11}(t)\cdot\boldsymbol{e}_{\mathrm{m},0} + \boldsymbol{\Phi}_{12}(t)\cdot\dot{\boldsymbol{e}}_{\mathrm{m},0}\\ &+ \int_0^t \boldsymbol{\Phi}_{12}(t-\tau)\cdot\widetilde{\boldsymbol{R}}_{\mathrm{m}}(\tau)d\tau,\end{aligned}$$

with $\boldsymbol{\Phi}_{11}$ and $\boldsymbol{\Phi}_{12}$ being the upper left / right part of the fundamental matrix and

$$\widetilde{\boldsymbol{R}}_{\mathrm{m}} = \boldsymbol{M}_{\mathrm{e}}^{-1}\boldsymbol{R}_{\mathrm{m}}. \tag{5}$$

With the bounds $\widetilde{C}_{11}(t) \geq \|\boldsymbol{\Phi}_{11}(t)\|_{\boldsymbol{G}_{\mathrm{m}}}$ and $\widetilde{C}_{12}(t) \geq \|\boldsymbol{\Phi}_{12}(t)\|_{\boldsymbol{G}_{\mathrm{m}}}$, the error bound

$$\begin{aligned}\widetilde{\triangle}_{\mathrm{q}}(t) &:= \widetilde{C}_{11}(t)\|\boldsymbol{e}_{m,0}\|_{\boldsymbol{G}_{\mathrm{m}}} + \widetilde{C}_{12}(t)\|\dot{\boldsymbol{e}}_{\mathrm{m},0}\|_{\boldsymbol{G}_{\mathrm{m}}}\\ &+ \int_0^t \widetilde{C}_{12}(t-\tau)\|\widetilde{\boldsymbol{R}}_{\mathrm{m}}(\tau)\|_{\boldsymbol{G}_{\mathrm{m}}}d\tau\end{aligned} \tag{6}$$

was first derived and later changed to

$$\begin{aligned}\triangle_{\mathrm{q}}(t) &:= C_{11}\|\boldsymbol{e}_{\mathrm{m},0}\|_{\boldsymbol{G}_{\mathrm{m}}} + C_{12}\|\dot{\boldsymbol{e}}_{\mathrm{m},0}\|_{\boldsymbol{G}_{\mathrm{m}}}\\ &+ C_{12}\int_0^t \|\widetilde{\boldsymbol{R}}_{\mathrm{m}}(\tau)\|_{\boldsymbol{G}_{\mathrm{m}}}d\tau\end{aligned} \tag{7}$$

with the constants C_{11}, C_{12} being independent of the current time step and $\boldsymbol{G}_{\mathrm{m}}$ being a weighting matrix usually chosen to be $\boldsymbol{M}_{\mathrm{e}}$ in the FE context. As error bounds, both satisfy

$$\|\boldsymbol{e}_{\mathrm{m}}(t)\|_{\boldsymbol{G}_{\mathrm{m}}} \leq \widetilde{\triangle}_{\mathrm{q}}(t) \leq \triangle_{\mathrm{q}}(t).$$

Similarly, error bounds for the output

$$\|\boldsymbol{y}(t) - \bar{\boldsymbol{y}}(t)\|_2 \leq \widetilde{\triangle}_{\mathrm{y}}(t) \leq \triangle_{\mathrm{y}}(t).$$

can be calculated by

$$\widetilde{\triangle}_{\mathrm{y}}(t) := C_2\widetilde{\triangle}_{\mathrm{q}}(t) \tag{8}$$

$$\triangle_{\mathrm{y}}(t) := C_2\triangle_{\mathrm{q}}(t) \tag{9}$$

with the constant

$$C_2 \geq \|\boldsymbol{C}_{\mathrm{e}}\|_{\boldsymbol{G}_{\mathrm{m}},2} := \max_{\|\boldsymbol{z}\|_{\boldsymbol{G}_{\mathrm{m}}}=1} \|\boldsymbol{C}_{\mathrm{e}}\boldsymbol{z}\|_2.$$

There are several advantages in using this specific error estimator. First of all, it is based on work by Haasdonk and Ohlberger (2011) for first order systems but the estimators (6) and (7) were derived specifically for second order systems (2). Second of all, the error estimator can be applied to any Galerkin reduction. This makes the aforementioned error estimator an ideal tool for practical usage in simulation software. We will show in Section 5 how it can be easily deployed in a non-intrusive fashion. Thirdly, it has potential for improvements which will be presented in the next section.

3.2 Speedup of Error Estimator

The error estimator is based upon the spectral norm of a matrix $\boldsymbol{\Phi}$ which consists of computing the maximum singular value of $\boldsymbol{\Phi}$ or – equivalently – the maximum eigenvalue of $\boldsymbol{\Phi}^T\boldsymbol{\Phi}$. Usually, iterative methods like the Lanczos or Arnoldi algorithms are used to efficiently compute a Krylov subspace for the approximation of the maximum eigenvalue of $\boldsymbol{\Phi}^T\boldsymbol{\Phi}$, see Sorensen (1996). These algorithms are more advanced than the power iteration, see Saad (2003). Therefore, the numerical spectral norm will be an approximation up to a given accuracy and the convergence rate differs from matrix to matrix.

We propose and analyze four alternatives to approximate $\|\boldsymbol{\Phi}\|_{\boldsymbol{G}_{\mathrm{m}}}$ in order to get a fixed computational complexity, faster calculation and better scaling for large systems. The results are summarized in Table 1 for the same simulation environment described in Section 4.

- The first two approximations are based on the upper bounds $\|\boldsymbol{\Phi}\|_2 \leq \|\boldsymbol{\Phi}\|_{\mathrm{Fro}}$ and $\|\boldsymbol{\Phi}\|_2 \leq \sqrt{\|\boldsymbol{\Phi}\|_1\|\boldsymbol{\Phi}\|_\infty}$, see (Golub and van Loan, 2013, Chapter 2.3). In presence of the scaling matrix $\boldsymbol{G}_{\mathrm{m}}$, this leads to

$$\begin{aligned}\|\boldsymbol{\Phi}\|_{\boldsymbol{G}_{\mathrm{m}}} &= \sup_{\boldsymbol{z}\neq\boldsymbol{0}} \frac{\|\boldsymbol{\Phi}\boldsymbol{z}\|_{\boldsymbol{G}_{\mathrm{m}}}}{\|\boldsymbol{z}\|_{\boldsymbol{G}_{\mathrm{m}}}} = \sup_{\boldsymbol{z}\neq\boldsymbol{0}} \frac{\|\boldsymbol{G}_{\mathrm{m}}^{\frac{1}{2}}\boldsymbol{\Phi}\boldsymbol{z}\|_2}{\|\boldsymbol{G}_{\mathrm{m}}^{\frac{1}{2}}\boldsymbol{z}\|_2}\\ &\overset{\boldsymbol{w}=\boldsymbol{G}_{\mathrm{m}}^{\frac{1}{2}}\boldsymbol{z}}{=} \sup_{\boldsymbol{w}\neq\boldsymbol{0}} \frac{\|\boldsymbol{G}_{\mathrm{m}}^{\frac{1}{2}}\boldsymbol{\Phi}\boldsymbol{G}_{\mathrm{m}}^{-\frac{1}{2}}\boldsymbol{w}\|_2}{\|\boldsymbol{w}\|_2} = \|\boldsymbol{G}_{\mathrm{m}}^{\frac{1}{2}}\boldsymbol{\Phi}\boldsymbol{G}_{\mathrm{m}}^{-\frac{1}{2}}\|_2.\end{aligned}$$

  Then it follows:

$$\|\boldsymbol{\Phi}\|_{\boldsymbol{G}_\mathrm{m}} \leq \|\boldsymbol{G}_\mathrm{m}^{\frac{1}{2}}\boldsymbol{\Phi}\boldsymbol{G}_\mathrm{m}^{-\frac{1}{2}}\|_\mathrm{Fro} \text{ and} \tag{10}$$

$$\leq \sqrt{\|\boldsymbol{G}_\mathrm{m}^{\frac{1}{2}}\boldsymbol{\Phi}\boldsymbol{G}_\mathrm{m}^{-\frac{1}{2}}\|_1 \|\boldsymbol{G}_\mathrm{m}^{\frac{1}{2}}\boldsymbol{\Phi}\boldsymbol{G}_\mathrm{m}^{-\frac{1}{2}}\|_\infty} \tag{11}$$

Both approximations (10) and (11) have the advantage of a fixed computational complexity but only (10) shows a moderate speedup together with a small overestimation compared to the original norm $\|\boldsymbol{\Phi}\|_{\boldsymbol{G}_\mathrm{m}}$, see Table 1.

- Both, the direct computation of $\|\boldsymbol{\Phi}\|_{\boldsymbol{G}_\mathrm{m}}$ and the approximation with (10) and (11), need powers of $\boldsymbol{G}_\mathrm{m}$ which need to be pre-computed in the offline step. This is impractical for large matrices. Computation of the inverse and matrix square root not only leads to large computation times but also results in dense matrices taking up much memory. Therefore, the computation of $\|\boldsymbol{\Phi}\|_2$ is traced back to a generalized eigenvalue problem:

$$\begin{aligned}\|\boldsymbol{\Phi}\|_{\boldsymbol{G}_\mathrm{m}} &= \|\boldsymbol{G}_\mathrm{m}^{\frac{1}{2}}\boldsymbol{\Phi}\boldsymbol{G}_\mathrm{m}^{-\frac{1}{2}}\|_2 = \sigma_\mathrm{max}(\boldsymbol{G}_\mathrm{m}^{\frac{1}{2}}\boldsymbol{\Phi}\boldsymbol{G}_\mathrm{m}^{-\frac{1}{2}}) \\ &= \sqrt{\lambda_\mathrm{max}(\boldsymbol{G}_\mathrm{m}^{-\frac{1}{2}}\boldsymbol{\Phi}^\mathrm{T}\boldsymbol{G}_\mathrm{m}\boldsymbol{\Phi}\boldsymbol{G}_\mathrm{m}^{-\frac{1}{2}})} \\ &= \sqrt{\lambda_\mathrm{max}(\boldsymbol{G}_\mathrm{m}^{-1}\boldsymbol{\Phi}^\mathrm{T}\boldsymbol{G}_\mathrm{m}\boldsymbol{\Phi})} \\ &= \sqrt{\lambda_\mathrm{max}(\boldsymbol{\Phi}^\mathrm{T}\boldsymbol{G}_\mathrm{m}\boldsymbol{\Phi}, \boldsymbol{G}_\mathrm{m})}\end{aligned} \tag{12}$$

Here we used the symmetry of $\boldsymbol{G}_\mathrm{m}$, the equality $\sigma_\mathrm{max}(\boldsymbol{\Psi}) = \sqrt{\lambda_\mathrm{max}(\boldsymbol{\Psi}^\mathrm{T}\boldsymbol{\Psi})}$, equivalence of the spectrum of similar matrices, and defined $\lambda_\mathrm{max}(\boldsymbol{\Phi}, \boldsymbol{\Psi})$ as the maximum eigenvalue of the generalized eigenvalue problem

$$\boldsymbol{\Phi}\boldsymbol{x} = \lambda\boldsymbol{\Psi}\boldsymbol{x}. \tag{13}$$

The computation of (12) does not involve any direct matrix inversion by using the Implicitly Restarted Arnoldi Method, which is also implemented in Matlab via the ARPACK package, see Lehoucq et al. (1998). Therefore, the norm $\|\boldsymbol{\Phi}\|_{\boldsymbol{G}_\mathrm{m}}$ can be also computed for very large matrices in reasonable time. This can be seen in the benchmark test presented in Table 1.

- If $\boldsymbol{G}_\mathrm{m}$ is well-conditioned, one can also use the approximation $\|\boldsymbol{\Phi}\|_{\boldsymbol{G}_\mathrm{m}} \leq \sqrt{\mathrm{cond}(\boldsymbol{G}_\mathrm{m})}\|\boldsymbol{\Phi}\|_2$ since

$$\begin{aligned}\|\boldsymbol{\Phi}\|_{\boldsymbol{G}_\mathrm{m}} &= \|\boldsymbol{G}_\mathrm{m}^{\frac{1}{2}}\boldsymbol{\Phi}\boldsymbol{G}_\mathrm{m}^{-\frac{1}{2}}\|_2 \leq \|\boldsymbol{G}_\mathrm{m}^{\frac{1}{2}}\|_2\|\boldsymbol{\Phi}\|_2\|\boldsymbol{G}_\mathrm{m}^{-\frac{1}{2}}\|_2 \\ &= \sqrt{\sigma_\mathrm{max}(\boldsymbol{G}_\mathrm{m})}\|\boldsymbol{\Phi}\|_2(\sqrt{\sigma_\mathrm{min}(\boldsymbol{G}_\mathrm{m})})^{-1} \\ &= \sqrt{\mathrm{cond}(\boldsymbol{G}_\mathrm{m})}\|\boldsymbol{\Phi}\|_2.\end{aligned} \tag{14}$$

As with (12), it does not involve any matrix inversion in the online step but leads to high overestimation due to the dependence on the condition number of $\boldsymbol{G}_\mathrm{m}$, see Table 1.

In summary, our alternatives (10) and (12) for the computation of the error bound led to high speedup with only small overestimation in comparison to the original method introduced in Ruiner et al. (2012). The solution of the generalized eigenvalue problem (12) will be used in the following experiments.

4. SENSITIVITY ANALYSIS

The sensitivity of the error estimator is of great interest if we want to generalize its properties to other models and inputs. Since the error estimator is only able to estimate the error in the elastic degrees of freedom of one body, only the first arm of the slender robot arm example is considered as a single linear FE body excited with $\boldsymbol{F} = 10\sin(2\pi t/\mathrm{s})$ N in the neg. y-direction at the right end of the first arm. The second arm is not considered first. We use the reorthogonalization as suggested by Buhr et al. (2014) to achieve better results along with the following reduction methods:

Table 1. Comparison of the alternatives for computing $\|\boldsymbol{\Phi}\|_{\boldsymbol{G}_\mathrm{m}}$ as described in Section 3.2. The values are relative to $\|\boldsymbol{\Phi}\|_{\boldsymbol{G}_\mathrm{m}}$ and for the estimator (6) with POD reduction.

substitution for $\|\boldsymbol{\Phi}\|_{\boldsymbol{G}_\mathrm{m}}$	(10)	(11)	(12)	(14)
speedup	2.6	1.2	4.6	6.0
overestimation	1.2 %	135 %	0.0 %	1178 %

- CMS-Gram according to Holzwarth and Eberhard (2015) which is an extension of Component Mode Synthesis where the internal dynamics are reduced to 30 degrees of freedom with frequency weighted balanced truncation in the frequency range $[0, 20]$ Hz,
- Krylov reduction to the dimension 15 with 15 shifts equidistantly chosen between $0i$ and $35i$,
- second order Gramian matrix reduction techniques as described in Fehr (2011) where the computation of frequency weighted Gramian matrices are calculated with POD based on 20 snapshots in the frequency range $[0, 200]$ Hz to the dimension 7.

First, we investigate the performance of the error estimator for these three reduction methods. As shown in Fig. 4, POD leads to an error estimator several orders smaller than Krylov or CMS-Gram for a SOLID 185 formulation. In addition, the same experiments were run for the same setup modeled now with the 2D plane stress element PLANE 182. Since the error estimator for a PLANE 182 formulation behaves almost identical to the SOLID 185, we will present our analysis only for one of these elements and keep in mind that they are valid for both. This shows that the error estimator is insensitive to different modeling approaches. I a very first approach a SHELL 181 formulation (finite strain shell) was used. However, the error bound was much higher due to the ill-conditioning of the system matrices of the SHELL 181 model.

In Fig. 5, the real errors (solid lines) are compared with the error bounds (dashed lines) for one output chosen at the tip (y-axis) of the beam. Not only is the error bound, defined in (8), very low with a value of 10^{-7} for POD-Gram but it also follows almost perfectly the real error. The small underestimations of some peaks are due to numerical errors, e.g., during integration in (6). In contrast, the error of the CMS-Gram and Krylov reduction are overestimated by several orders. The error bound is even larger than the maximum amplitude of the output.

It is also of great interest how sensitive the error estimator is against a change in the input and the model itself. For this, a Krylov reduction of size 10 as described above is applied to one PLANE 182 beam with different amplitudes (10 N to 100 N) and frequencies (1 Hz to 10 Hz) of the excitation force. Figure 6 shows that the frequency has a much higher impact on the error estimator than the amplitude. The higher the frequency, the higher the error bound. The slenderness ratio is defined as quotient of the

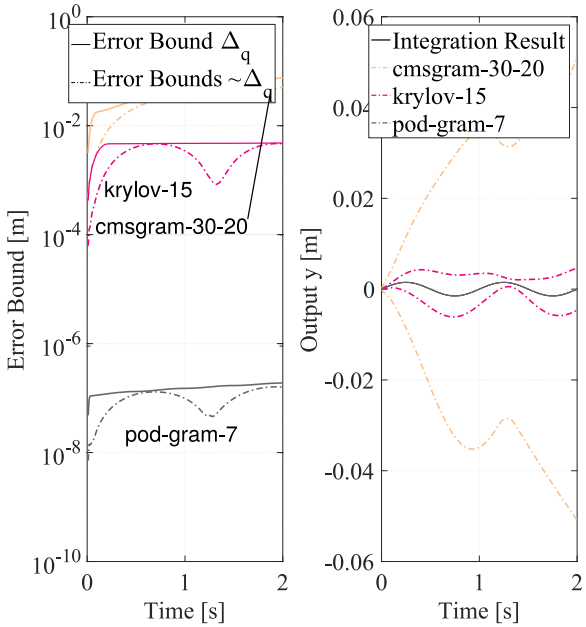

Fig. 4. State error bounds and comparison with reduced simulation for SOLID 185.

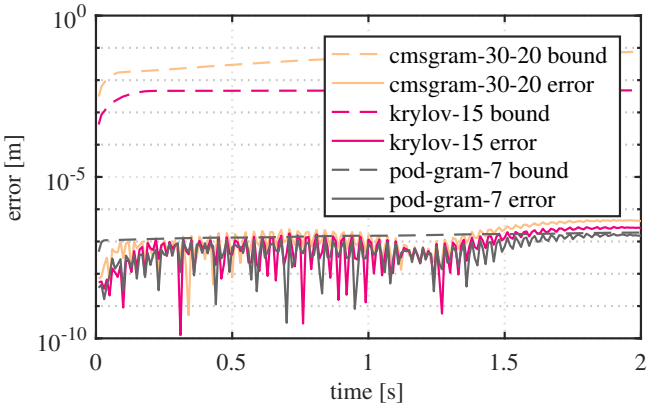

Fig. 5. Comparison of error bound and real error for SOLID 185 at one output.

length and width of the beam. As seen in Figure 7, the results vary by two orders but are not monotonic regarding the slenderness ratio (5 to 100). A quotient of 20 : 1 seems to be optimal for this model.

In summary, the error estimator is only moderately sensitive against a change in the input or the model itself. This allows to generalize results qualitatively to other models. However, it is sensitive to numeric noise, e.g., the experiment with the SHELL 181 formulation failed due to the condition number of $\boldsymbol{M}_\mathrm{e}$ and the multiple reorthogonalization by Buhr et al. (2014) had an influence. Since the error estimator is highly sensitive to the reduction method, analyses of the estimator are only valid for one specific MOR method. We also showed that the overestimation can be arbitrarily small as seen in the case of POD (black line in Fig. 4), which was also not known before.

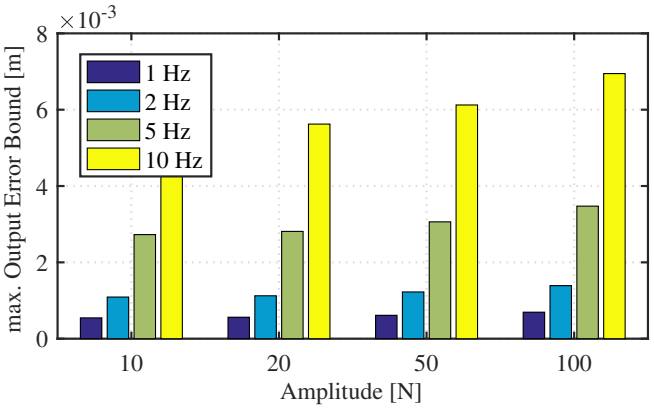

Fig. 6. Sensitivity study of PLANE 182 regarding the excitation force.

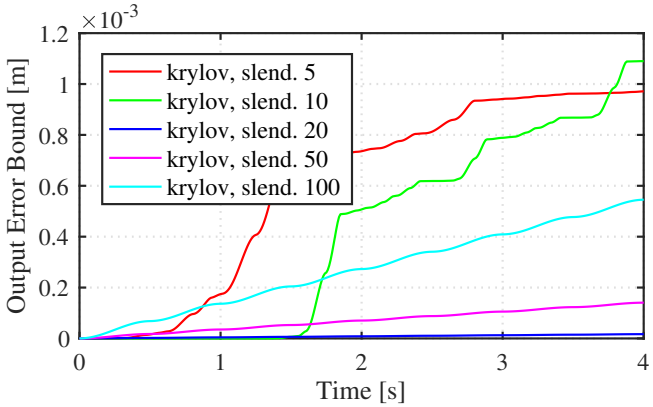

Fig. 7. Sensitivity study of PLANE 182 regarding the slenderness ratio.

5. ERROR ESTIMATION WITHIN AN EMBS PROGRAM PACKAGE

In this section, we will show that the error estimator of Ruiner et al. (2012) can be implemented non-intrusively, i.e., only with a few changes in the used simulation environment. In our case, this is Neweul-M^2.

In order to allow for a smooth extension of the error estimator to Neweul-M^2, it is implemented as an external, i.e., independent Matlab class. During the creation of the class, the system matrices, simulation details like the initial values, and options are given as inputs to the computation of the offline quantities from Ruiner et al. (2012). For the online phase, the method `calcErrorOnline` of the error estimator class is given to the function handle `OutputFcn` of Neweul-M^2, which serves the same purpose as for the Matlab solvers: After each successful time step in the simulation, the `OutputFcn` (in our case `calcErrorOnline`) is called with the current time and state as input. The error estimator class then computes the error in the state and output from these inputs and the offline quantities. The error bounds are then saved as class properties and can be used later for post-processing. This parallel calculation of the error estimator only lengthens the simulation time by 3 %, e.g., 6.2 s instead of 6.0 s for the PLANE 182 model.

The error estimator class provides several options to control the level of offline approximation, the way constants

in the residual integral will be approximated, and which of the norm approximations from above should be used.

This way, not a single line in Neweul-M^2 needs to be changed in order to use the error estimator during the reduced simulation. Therefore, the error estimator class can easily be used with other simulation software when a similar interface exists. Additionally, the use of a function hook of the solver allows to stop the simulation if the error estimator becomes larger than a threshold defined by the user. This also allows for refinement of the reduction basis.

It is also possible to use bases generated by the MOR package RBmatlab in combination with Neweul-M^2 and the activated error estimator. For symplectic bases sizes between 2 and 30, errors between 10^{-6} to 10^{-8} were accomplished for the one beam PLANE 182 model. The error estimator only achieved a bound of 10^1 to 10^0.

6. CONCLUSIONS AND FUTURE WORK

The error estimator of Ruiner et al. (2012) is applicable to every second-order mechanical system and every Galerkin reduction based MOR method. Despite of its generality, the estimator also had some downsides and unknown properties which we investigated. First, we sped up the calculation by a factor of 4.6 with an immeasurable additional overestimation. We then performed a sensitivity analysis which showed only moderate dependence on the model and inputs but high dependence on the used reduction method. This gave us further insight for the future deployment of the error estimator to other models. We also accomplished to find an example with almost no overestimation, which shows the potential of the error estimator. Lastly, we described a way to implement the error estimator in a non-intrusive way for existing simulation software.

Future work may investigate why the overestimation varies this much amongst different MOR methods. Additionally, the error estimator of Ruiner et al. (2012) cannot be applied to multibody systems directly but only to the elastic degrees of freedom of one body. Therefore, an extension based on the nonlinear coupling forces, given as nonlinear input, needs to be carefully investigated and further development is needed. Sensitivity studies and further analytical research is in preparation for later publication. Even though we were able to speed up the error estimation process, it is still infeasible to compute the constants C_{11} and C_{12} in the offline step for large systems. Analytical bounds need to be found.

REFERENCES

Bhatt, A., Fehr, J., and Haasdonk, B. (2017). Model order reduction of an elastic body under large rigid motion. In A.F. Radu and I. Berre (eds.), *Proceedings 12th European Conference on Numerical Mathematics and Advanced Applications, ENUMATH 2017, submitted.*

Buhr, A., Engwer, C., Ohlberger, M., and Rave, S. (2014). A numerically stable a posteriori error estimator for reduced basis approximations of elliptic equations. In E.O. XO and A. Huerta (eds.), *Proceedings 11th World Congress on Computational Mechanics, WCCM 2014, 5th European Conference on Computational Mechanics, ECCM 2014 and 6th European Conference on Computational Fluid Dynamics, ECFD 2014.*

Fehr, J. (2011). *Automated and Error-Controlled Model Reduction in Elastic Multibody Systems.* Dissertation, Schriften aus dem Institut für Technische und Numerische Mechanik der Universität Stuttgart, Vol. 21. Shaker Verlag, Aachen.

Fehr, J., Grunert, D., Holzwarth, P., Frhlich, B., Walker, N., and Eberhard, P. (2017). Morembs a model order reduction package for elastic multibody systems and beyond. In *KoMSO Challenge Workshop on Reduced-Order Modeling for Simulation and Optimization.* Springer. (accepted for publication, 25 pages).

Golub, G.H. and van Loan, C.F. (2013). *Matrix Computations.* The Johns Hopkins University Press, Baltimore, 4 edition.

Gubisch, M. and Volkwein, S. (2017). Proper orthogonal decomposition for linear-quadratic optimal control. In P. Benner, M. Ohlberger, A. Cohen, and K. Willcox (eds.), *Model reduction and approximation : theory and algorithms*, 3–64. SIAM, Society for Industrial and Applied Mathematics.

Haasdonk, B. (2017). Reduced basis methods for parametrized PDEs – a tutorial introduction for stationary and instationary problems. In P. Benner, A. Cohen, M. Ohlberger, and K. Willcox (eds.), *Model Reduction and Approximation: Theory and Algorithms*, 65–136. SIAM, Philadelphia.

Haasdonk, B. and Ohlberger, M. (2011). Efficient reduced models and a-posteriori error estimation for parametrized dynamical systems by offline/online decomposition. *Mathematical and Computer Modelling of Dynamical Systems*, 17(2), 145–161. doi: 10.1080/13873954.2010.514703.

Holzwarth, P. and Eberhard, P. (2015). SVD-based improvements for component mode synthesis in elastic multibody systems. *European Journal of Mechanics A/Solids*, 49, 408–418.

Kurz, T., Eberhard, P., Henninger, C., and Schiehlen, W. (2010). From Neweul to Neweul-M^2: Symbolical equations of motion for multibody system analysis and synthesis. *Multibody System Dynamics*, 24(1), 25–41.

Lehoucq, R.B., Sorensen, D.C., and Yang, C. (1998). *ARPACK Users' Guide: Solution of Large Scale Eigenvalue Problems with Implicitly Restarted Arnoldi Methods.* SIAM, Philadelphia.

Maboudi Afkham, B. and Hesthaven, J.S. (2017). Structure preserving model reduction of parametric Hamiltonian systems. *SIAM Journal on Scientific Computing.* Accepted for publication.

Panzer, H.K.F. (2014). *Model Order Reduction by Krylov Subspace Methods with Global Error Bounds and Automatic Choice of Parameters.* Dissertation, Technische Universität München. Verlag Dr. Hut, München.

Ruiner, T., Fehr, J., Haasdonk, B., and Eberhard, P. (2012). A-posteriori error estimation for second order mechanical systems. *Acta Mechanica Sinica*, 28(3), 854–862. doi:10.1007/s10409-012-0114-7.

Saad, J. (2003). *Iterative Methods for Sparse Linear Systems.* SIAM, Philadelphia, 2 edition.

Sorensen, D. (1996). Implicitly restarted Arnoldi/Lanczos methods for large scale eigenvalue calculations. Technical report, Institute for Computer Applications in Science and Engineering (ICASE).